Upregulation of Epac1 Promotes Pericyte Loss by Inducing Mitochondrial Fission, Reactive Oxygen Species Production, and Apoptosis

Wenli Yang,[1,2] Fan Xia,[3] Fang Mei,[1,2] Shuizhen Shi,[3] William G. Robichaux III,[1,2] Wei Lin,[1,2] Wenbo Zhang,[3,4] Hua Liu,[3] and Xiaodong Cheng[1,2]

[1]Department of Integrative Biology and Pharmacology, University of Texas Health Science Center, Houston, Texas, United States
[2]Texas Therapeutics Institute, University of Texas Health Science Center, Houston, Texas, United States
[3]Department of Ophthalmology & Visual Sciences, University of Texas Medical Branch, Galveston, Texas, United States
[4]Department of Neurobiology, University of Texas Medical Branch, Galveston, Texas, United States

Correspondence: Hua Liu, Department of Ophthalmology & Visual Sciences, University of Texas Medical Branch, 301 University Boulevard, Galveston, TX 77555-0144, USA; hualiu@utmb.edu.
Xiaodong Cheng, Department of Integrative Biology and Pharmacology, University of Texas Health Science Center, 6431 Fannin Street, Houston, TX 77030, USA; xiaodong.cheng@uth.tmc.edu.

WY and FX contributed equally to this work.

Received: March 30, 2023
Accepted: August 9, 2023
Published: August 31, 2023

Citation: Yang W, Xia F, Mei F, et al. Upregulation of Epac1 promotes pericyte loss by inducing mitochondrial fission, reactive oxygen species production, and apoptosis. *Invest Ophthalmol Vis Sci.* 2023;64(11):34. https://doi.org/10.1167/iovs.64.11.34

Purpose. The pathogenic mechanisms behind the development of ischemic retinopathy are complex and poorly understood. This study investigates the involvement of exchange protein directly activated by cAMP (Epac)1 signaling in pericyte injury during ischemic retinopathy, including diabetic retinopathy, a disease that threatens vision.

Methods. Mouse models of retinal ischemia–reperfusion injury and type 1 diabetes induced by streptozotocin were used to investigate the pathogenesis of these diseases. The roles of Epac1 signaling in the pathogenesis of ischemic retinopathy were determined by an Epac1 knockout mouse model. The cellular and molecular mechanisms of Epac1-mediated pericyte dysfunction in response to high glucose were investigated by specific modulation of Epac1 activity in primary human retinal pericytes using Epac1-specific RNA interference and a pharmacological inhibitor.

Results. Ischemic injury or diabetes-induced retinal capillary degeneration were associated with an increased expression of Epac1 in the mouse retinal vasculature, including both endothelial cells and pericytes. Genetic deletion of Epac1 protected ischemic injury-induced pericyte loss and capillary degeneration in the mouse retina. Furthermore, high glucose-induced Epac1 expression in retinal pericytes was accompanied by increased Drp1 phosphorylation, mitochondrial fission, reactive oxygen species production, and caspase 3 activation. Inhibition of Epac1 via RNA interference or pharmacological approaches blocked high glucose-mediated mitochondrial dysfunction and caspase 3 activation.

Conclusions. Our study reveals an important role of Epac1 signaling in mitochondrial dynamics, reactive oxygen species production, and apoptosis in retinal pericytes and identifies Epac1 as a therapeutic target for treating ischemic retinopathy.

Keywords: diabetic retinopathy, cyclic AMP, exchange protein directly activated by cAMP (Epac)1, pericyte, mitochondrial fission

Ischemic retinopathy, including diabetic retinopathy (DR), is a vision-threatening disease. Clinically, it is characterized by a period of retinal ischemia caused by retinal capillary degeneration, vessel occlusion, or retarded vessel growth, followed by neovascularization and microaneurysms, resulting in hemorrhages, leakage, and swelling of the neuroretinal tissue. These changes ultimately lead to a decline in visual acuity and even blindness.[1–5] At the cellular level, maladaptive inflammation in response to stress conditions such as hyperglycemia and ischemia instigates the production of inflammatory mediators and reactive oxygen species (ROS), which causes a cascade of events leading to retinal vascular dysfunction, degeneration, and ultimately retinal neovascularization (pathological angiogenesis). The pathogenic mechanisms underpinning the development of ischemic retinopathy seem to be multifactorial and remain incompletely understood, and current treatments have significant limitations.[6,7] Abnormal neovascularization is a hallmark of proliferative retinopathy; therapy with anti-VEGF drugs has become one of the gold standard treatments for ischemic retinopathy. Although anti-VEGFs demonstrate modest clinical benefits, these drugs fail to fully attenuate clinical progression or reverse damage to the retina and have to be administered frequently via invasive intravitreal injections over many years.[8] Thus, a better understanding of ischemic retinopathy's etiology and molecular mechanisms is urgently needed to develop novel mechanism-based therapeutics for this devastating disease.

The prototypic second messenger, cAMP, is a major stress-response signal that plays a crucial role in various biological

processes under physiological and pathological conditions. In animals, the effects of cAMP are mainly transduced by two ubiquitously expressed intracellular cAMP receptors, protein kinase A and the exchange protein directly activated by cAMP (Epac).[9] In mammals, two isoforms of Epac exist, Epac1 and Epac2, which are products of independent genes.[10,11] Although Epac1 and Epac2 share significant sequence homology and similar biochemical properties, their physiological functions are mostly nonredundant owing to their distinct tissue distributions and ability to form discrete signalosomes with specific cellular partners.[12–15] Epac1 is more highly abundant than Epac2 in blood vessels.[16] Multiple reports demonstrate that the expression of Epac1 is upregulated in response to vascular injuries and promotes stenosis and atherogenesis in various independent animal models.[17–20] Our recent studies reveal that hyperactivation of Epac1 under pathological conditions promotes retinal neovascularization by accelerating VEGF signaling while suppressing the Notch pathway in endothelial cells (ECs).[21] Although Epac1 is dispensable for retinal vasculature development, that is physiological angiogenesis, genetic deletion or pharmacological inhibition of Epac1 leads to robust reductions in pathological neovascularization and avascular area in the retina in a mouse model of oxygen-induced retinopathy.[21]

In addition to the contribution of ECs, mural cells, including pericytes, play an important role in normal vascular development,[22,23] as well as in vascular remodeling in ischemic retinopathy.[24] The loss of pericytes represents the earliest morphologic change in a diabetic retina.[24–28] This process is accompanied by increased retinal capillary cell apoptosis and the formation of acellular capillaries and pericyte ghosts, which are early signs of retinopathy in animal models of DR. The mechanisms of stress-mediated pericyte loss are not clear. Mitochondrial dysfunction and ROS induced by hyperglycemia may be critical in this process.[29–31] In this study, we investigated the roles of Epac1 signaling in pericyte injury in response to stress, using various ocular and Epac1 knockout (KO) mouse models and primary human retinal pericytes (HRPCs).

Methods

Mice

C57BL/6 wild type (WT) and Epac1$^{-/-}$ mice were maintained as described previously.[32,33] Animal care adhered to the ARVO Statement for the Use of Animals in Ophthalmic and Vision Research, and the Institutional Animal Care and Use Committee of the University of Texas Medical Branch approved the use of animals.

Retinal Ischemia–Reperfusion (IR) Model

As previously reported, the retinal IR model was established by transient elevation of intraocular pressure (IOP).[33] In short, 8- to 10-week-old mice were anesthetized with 75 mg/kg phenobarbital sodium by intraperitoneal injection, followed by topical application of 1% tropicamide, 2.5% phenylephrine, and 0.5% proparacaine hydrochloride in sequence for pupil dilation and local anesthesia. Mice were carefully placed on a warm pad to maintain their body temperature. A 30G infusion needle connected to a reservoir of sterile saline was inserted into the anterior chamber to create a 110-mm Hg pressure in the eye. The IOP elevation was maintained for 50 minutes to induce retinal injury.

Diabetic Mouse Model

Type 1 diabetes (DB) was induced in 8-week-old C57BL/6 mice following the standard methodology.[34,35] In brief, 75 mg/kg streptozotocin (STZ, Cat. S0130; Sigma-Aldrich, St. Louiks, MO, USA) was administered to mice fasted for 6 hours by intraperitoneal injection daily. STZ was dissolved in a freshly prepared 0.01 M citrate buffer and injected within 15 minutes. The blood glucose level was measured by a glucometer. Mice with blood glucose levels higher than 300 mg/dL were considered diabetic. Mice usually become diabetic after three to five injections. Mice were excluded from the study if they did not have DB after five injections. Age-matched and nondiabetic C57BL/6 mice were used as the controls.

Retinal Trypsin Digestion Assay

Mouse eyeballs were collected after euthanasia and fixed in 2% freshly prepared paraformaldehyde overnight. The next day, retinas were dissected, carefully cut into four petals, and digested in 3% trypsin at 37°C with gentle shaking for 5 to 6 hours. When digestion was sufficient, a soft brush was used to remove most of the neural tissue from the outer layer of the retina. Next, retinas were immersed in 0.5% Triton-X-100 for 30 minutes, and the neural residues were further flushed away by liquid drops. Isolated vasculatures were unfolded and dried on the slides to perform periodic acid-Schiff/hematoxylin staining. Eight images were taken at the mid-peripheral region for each sample using a 20× objective. Pericytes and acellular capillaries were counted from each image for quantification by examiners blinded to the mouse treatment or genotype.

Immunostaining of Retinal Vasculature

Mice were anesthetized and perfused with PBS to eliminate the blood from the retinal vasculatures. Eyeballs were collected for trypsin digestion, and isolated retinal vasculatures were fully unfolded and dried on the slides, followed by post-fixation with 4% paraformaldehyde for 10 minutes. After the fixative was removed by rinsing, the vasculatures were blocked with PBS containing 5% normal goat serum and 0.3% Triton-X-100 for 1 hour. Subsequently, the vasculatures were incubated with anti-Epac1 (Cat. 4155S; Cell Signaling Technology, Danvers, MA, USA), anti-NG2 (Cat. AB5320; MilliporeSigma, Burlington, MA, USA), and isolectin B4 (Cat. I21412; Invitrogen, Waltham, MA, USA) at 4°C overnight. The following day, the vasculatures were rinsed and incubated with Alexa Fluor 488- or 594-conjugated secondary antibodies at room temperature for 2 hours. Images were taken using confocal microscopy (LSM 800, Carl Zeiss Inc., Jena, Germany).

Cell Culture, Treatment, and Intracellular cAMP Determination

HRPCs (ACBRI 183) were from Cell Systems and cultured in 4N0-500 medium (Cell Systems, Kirkland, WA, USA) formulated at normal blood glucose level (low glucose [LG], 5 mM). Cell cultures were maintained in 5% CO_2 humidified

Investigative Ophthalmology & Visual Science

incubators at 37°C. HRPCs from passages between four and six were used for all experiments described in this study. Cells were seeded in 12-well or 6-well plates overnight. When cells reached 70% to 75% confluence, they were stimulated with high glucose (HG) (25 mM), with or without 30 minutes pretreatment of 5 µM Epac specific inhibitor ESI-09 (Cat. 406603; MedKoo Biosciences, Morrisville, NC, USA). Then the cells were harvested for protein or RNA analysis. For experiments involving RNA interference, HRPCs at 70% confluence were transfected with Epac1-specific Stealth RNAi small interfering RNA (siRNA) oligonucleotides (Cat. HSS115936) or negative control medium GC duplex (Cat. 462001) (Thermo Fisher Scientific, Waltham, MA, USA) at a final concentration of 50 nM using Lipofectamine 2000 (Thermo Fisher Scientific) according to the manufacturer's instructions. At 24 hours after transfection, cells were stimulated with HG for various specified intervals and harvested for further analyses. The intracellular cAMP of HRPCs treated with LG or HG was measured using a Direct cAMP ELISA kit (Cat. AD1-900-066A) from Enzo Biochem following the manufacturer's instructions. The relative cAMP level was normalized to protein concentration and expressed as fold changes over the LG control.

Real-time qPCR and Reverse Transcription (RT)-PCR

Total RNA from HRPCs treated with LG or HG for 16 hours was extracted with RNeasy Mini Kit (Qiagen, Hilden, Germany) according to the manufacturer's instructions. cDNA was prepared using a High Capacity Reverse Transcription kit (Applied Biosystems, Waltham, MA, USA). Real-time qPCR analysis was performed using iTaq Universal SYBR Green Supermix (Bio-Rad, Hercules, CA, USA) according to the manufacturers' recommendations. The qPCR primers for human Epac1 or Epac2 used were CCT CTC CAA CTC GGT GAA GC (forward) and CTG GCT GAA CAA CAC GGT C (reverse), or ATT AAT GGA CGC CTG TTT (forward) and CTC CTC AGG AAC AAA TCC A (reverse), respectively. The target amount ($2^{-\Delta\Delta CT}$) was obtained by normalizing to endogenous reference (GAPDH) and expressed as fold changes over the LG control. For RT-PCR of Epac1 transcript variants A and B, first-strand cDNAs of Epac1 transcript variants were synthesized with Oligo (dT) using purified total RNA extracted from HRPCs following the protocol of SuperScript III first-strand synthesis system. Subsequent PCRs were performed with specific primers for Epac1A (ATG AAG GTG GGC TGG CCA G [forward] and TCA TGG CTC CAG CTC TCG G [reverse]) and Epac1B (ATG GTG TTG AGA AGG ATG CAC CG [forward] and TCA TGG CTC CAG CTC TCG G [reverse]). Final RT-PCR products were analyzed by agarose gel electrophoresis.

Mitochondrial Fission Analysis

HRPCs were seeded on Attachment Factor (Cell Systems)-coated coverslips for at least 18 hours. The following day, the cells were treated with HG for 1.5 hours, with or without 5 µM ESI-09 pretreatment for 30 minutes. Mitochondria were stained using 100 nM MitoTracker Green FM (Cat. M7514, Invitrogen) together with Hoechst 33342 (10 µg/mL, Thermo Fisher Scientific) for additional 30 minutes (37°C, 5% CO_2) and imaged with Nikon A1R confocal imaging system. A minimum of 6 to 8 random fields of view were captured for each condition. Mitochondrial morphology was quantified as described previously[36] using ImageJ software (National Institutes of Health, Bethesda, MD, USA). In detail, all acquired images were background subtracted, filtered, thresholded, and binarized to identify mitochondrial segments. Continuous mitochondria structures were counted with the particle counting subroutine, and the number was normalized to the total mitochondrial area (sum of all pixels in the region of interest) to obtain the mitochondrial fragmentation count (Number of particles × 10,000/Total mitochondrial pixels) for each imaged cell. Randomly selected images ($n \geq 5$) were analyzed for each treatment group to calculate the respective mitochondrial fragmentation count values.

Cellular ROS Measurement

The levels of cellular ROS were monitored using a fluorescent probe dihydroethidium (DHE) (Cat. D11347, Thermo Fisher Scientific) following the manufacturer's instructions. HRPCs grown on the coverslips with HG (1 hour) treatments were loaded with 10 µM DHE at 37°C for 30 minutes. Images were acquired using Nikon A1R confocal microscopy at room temperature, and fluorescence intensity was measured and quantified for randomly selected cells ($n \geq 14$) using Image J software.

Western Blot Analysis

Upon various treatments, HRPCs were lysed in 1 × Cell Lysis Buffer (Cell Signaling Technology) supplemented with PMSF and cOmplete, Mini, EDTA-free Protease Inhibitor Cocktail Tablet (Roche, Basel, Switzerland). Cell lysates were resolved on 10% or 15% stain-free SDS-polyacrylamide gels containing 0.05% 2, 2, 2-trichloroethanol. After electrophoresis, images were documented by ChemiDoc Touch Imaging System (Bio-Rad) for total protein loading quantification before proteins were transferred to the Polyvinylidene fluoride membrane (Millipore). After blocking with 5% nonfat milk, the blots were incubated with primary antibodies against Epac1 clone 5D3 (Cat. 4155), phospho-DRP1 (Ser616) (Cat. 3455), DRP1 (D6C7) (Cat. 8570), cleaved caspase-3 (Asp175) (5A1E) (Cat. 9664), and GAPDH (Cat. 2118) (Cell Signaling Technology) at 4°C overnight, followed by incubation with horseradish peroxidase-conjugated secondary antibodies (Cat. 1706515 and Cat. 1706516, Bio-Rad). Proteins were detected using Amersham ECL Prime Western Blotting Detection Reagent (GE Healthcare Life Sciences, Chicago, IL, USA). The intensity of the signals was recorded with a ChemiDoc Touch Imaging System (Bio-Rad) and quantified with ImageJ or Image Lab 6.0.1 (Bio-Rad) software. Protein levels were first standardized against total protein loading or an internal control such as GAPDH. The final readout was normalized as a ratio of the protein levels of the sample group to those of the control group. Statistical analysis was performed using data from at least three independent experiments.

Statistics

Unless stated otherwise, all data were expressed as mean ± SEM and analyzed using the unpaired Student's *t* test with Welch's correction for comparison between two groups or ordinary one-way ANOVA Dunnett's multiple comparisons test with Geisser–Greenhouse correction for more than two

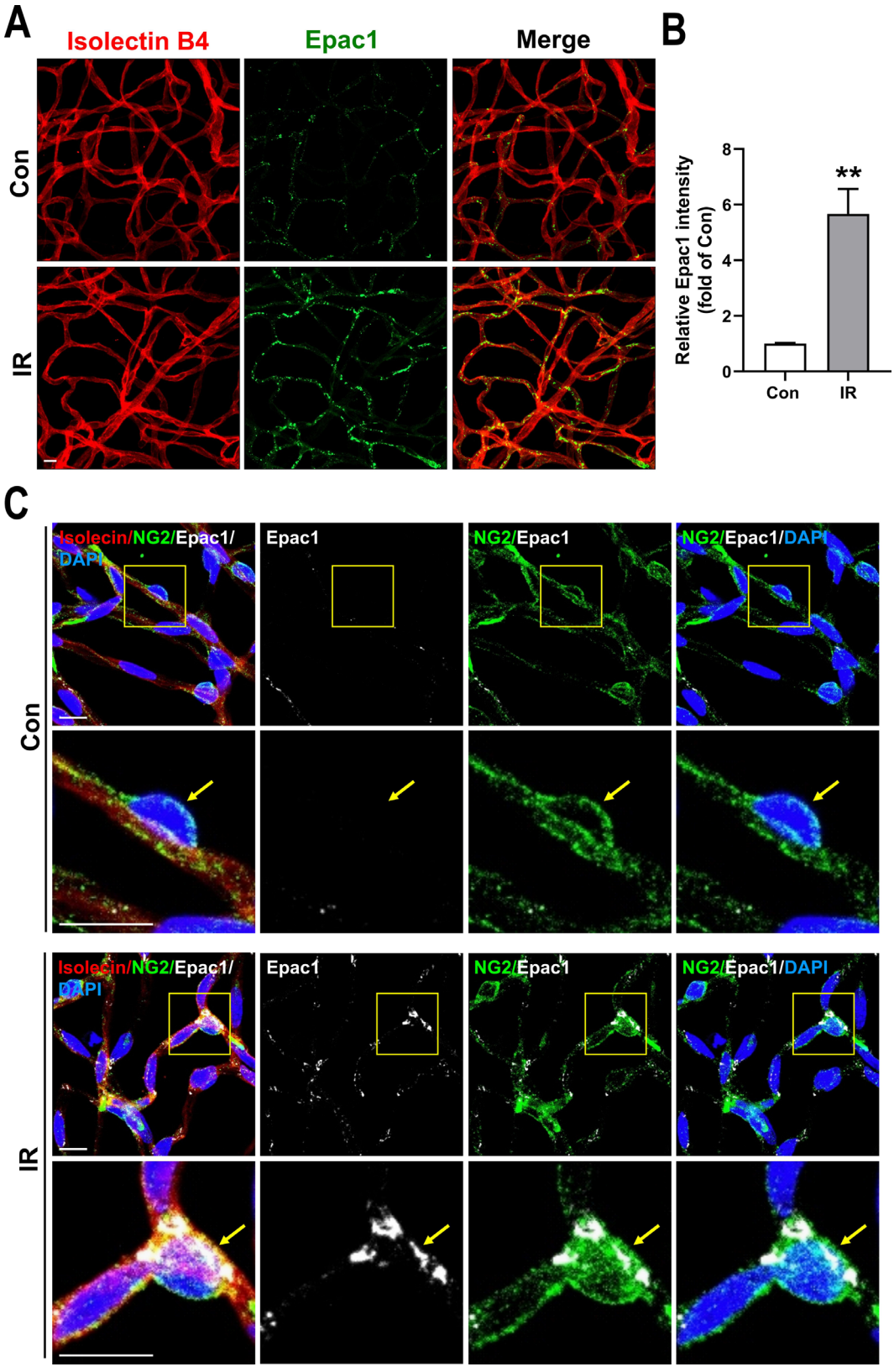

Figure 1. Epac1 expression is upregulated in the retinal vasculature after IR. WT mice were subjected to IR. Three days after IR, mice were perfused, eyeballs were collected, and the retinal vasculature was prepared by trypsin digestion. (**A**, **B**) Retinal vasculature was stained with anti-Epac1 (*green*) and isolectin B4 (red) for blood vessels. The graph represents the quantification of Epac1 expression in retinal vessels. (**C**) The retinal vasculature was stained with anti-Epac1 (*white*), anti-NG2 (*green*) for pericytes, isolectin B4 (*red*) for blood vessels, and DAPI (*blue*) for nuclei. The yellow arrow indicates pericyte. $^{**}P < 0.01$. $n = 4$. Scale bar, 10 µm.

Investigative Ophthalmology & Visual Science

groups. Differences were considered significant if $P < 0.05$. Cell culture experiments were repeated at least three times.

Results

Epac1 Upregulation Mediates Pericyte Loss and Capillary Degeneration in the Retinal Ischemia–Reperfusion Injury Model

As a critical stress response modulator, Epac1 has been shown to play essential roles in the development and progression of many pathogeneses,[15] and its expression is often upregulated in chronic disease conditions such as cancer,[37] heart failure,[38–40] chronic pain[41,42] and DB.[43] To investigate the potential involvement of Epac1 in ischemic retinopathy, we used a mouse model of retinal IR injury. This model, widely used to study retinal neuronal injury and vascular degeneration as seen in ischemic retinopathies including DR,[4,5,44,45] was induced by a transient increase of IOP to block retinal blood flow. After ischemia, the retina undergoes pathological changes such as retinal inflammation and neuronal cell death within a few hours to 1 week and vessel regression within 1 to 2 weeks.[5,44,45] In this model, we isolated retinal vasculatures by trypsin digestion for immunostaining. Epac1 expression was dramatically upregulated in the retinal vasculature at 3 days (Figs. 1A, B) and 7 days (data not shown) after ischemic injury. These results are consistent with prior reports that hypoxia-inducible factor 1α binds to the Epac1 promoter and promotes Epac1 protein expression during ischemia-induced tissue injuries.[46,47] The specificity of Epac1 staining was demonstrated by our data showing that Epac1 immunoreactivity was absent in retinal vessels from Epac1 KO mice (Supplementary Fig. S1). To examine if Epac1 is induced in pericytes, retinal vasculature was co-stained with pericyte marker NG2, which revealed that Epac1 expression was increased in pericytes after ischemic injury (Fig. 1C).

We further examined retinal vasculature in the IR model to investigate whether Epac1 is important for pericyte injury during vascular remodeling in ischemic retinopathy. Two weeks after ischemia, we performed retinal trypsin digestion to study retinal capillary degeneration. In this assay, pericytes are identified as round, dark extracapillary protrusions compared with ECs, which are oval and lighter in color. Acellular capillaries are defined as basement membrane tubes without nuclei.[48,49] We found that mice exposed to IR exhibited decreased pericytes and increased acellular capillary formation. Deleting Epac1 significantly decreased pericyte loss and the formation of acellular capillaries (Figs. 2A–C), indicating a pathological role of Epac1 in pericyte loss and vascular degeneration in the IR model.

Epac1 Expression and Capillary Degeneration Are Increased in the Retinal Vasculature of STZ-Induced Diabetic Mice

Encouraged by our finding that Epac1 expression is increased in the mouse retinal vasculature after IR (Fig. 1), we asked if Epac1 expression was similarly upregulated in a mouse model of STZ-induced type 1 DB. We injected STZ into C57BL/6 WT mice to induce DB (Supplementary Fig. S2). Three months after DB induction, retinas were collected from DB mice and age-matched nondiabetic control mice, and retinal vasculatures were isolated by trypsin digestion for immunostaining. We observed that Epac1 expression was significantly increased in the retinal vasculature of DB mice

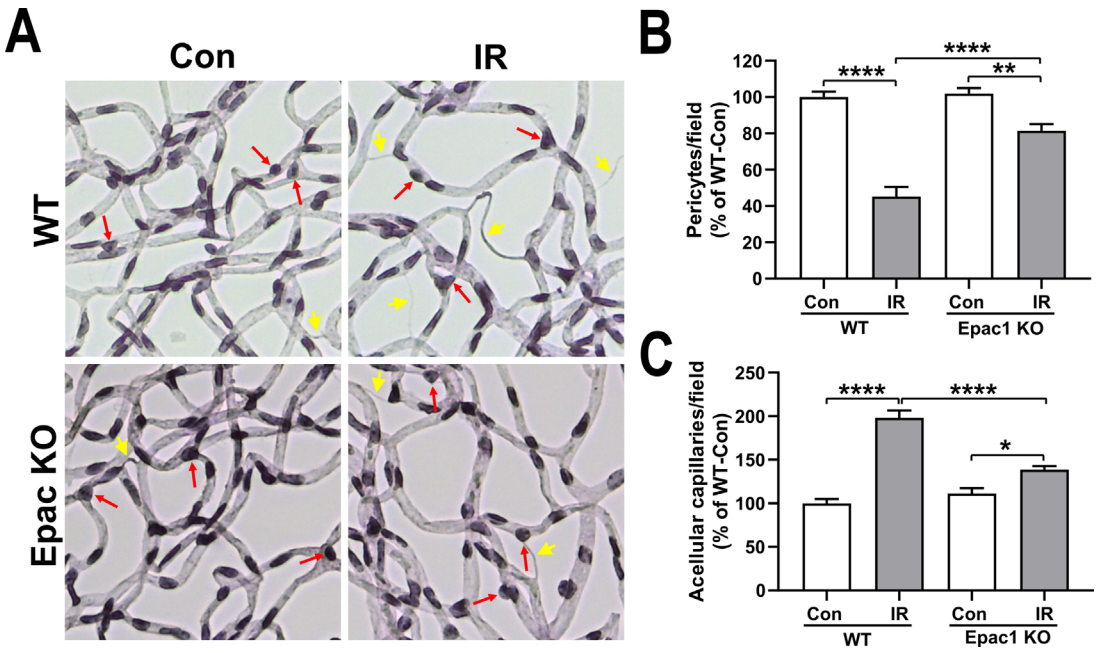

Figure 2. Epac1 deletion reduces IR-induced pericyte loss and capillary degeneration. WT and Epac1$^{-/-}$ mice were subjected to IR, eyeballs were collected 14 days after IR, and retinal trypsin digestion was performed. (**A**) Representative examples of retinal trypsin digests are shown. The *red arrows* indicate pericytes, identified by morphologic criteria (shape and relative position in the capillary), and the *yellow arrows* indicate acellular capillaries. (**B**, **C**) Quantification of the number of pericytes and acellular capillaries. *$P < 0.05$; **$P < 0.01$; ****$P < 0.0001$. $n = 4$–5.

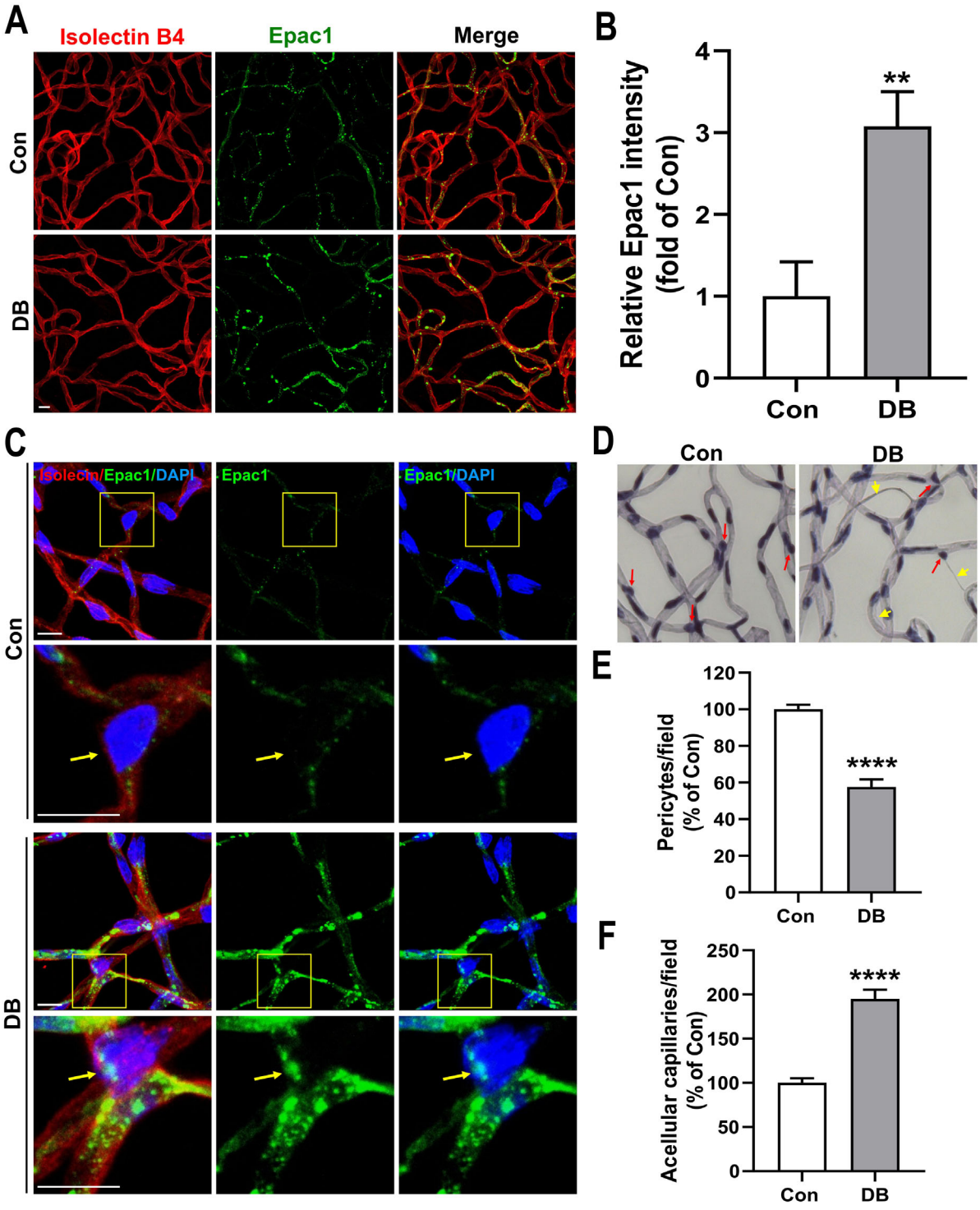

Figure 3. Diabetes upregulates Epac1 expression and induces capillary degeneration in the diabetic mouse retina. WT mice were injected with STZ to induce DB. (**A–C**) Mice were perfused, and eyeballs were collected three months after the induction of DB. The retinal vasculature was prepared by trypsin digestion and stained with anti-Epac1 (*green*) and isolectin B4 (*red*). Representative images of Epac1 expression in retinal vasculature are shown (**A**). The bar graph represents the quantification of Epac1 expression (**B**). Images are shown for the expression of Epac1 in the retinal pericytes (*yellow arrow*) of control and diabetic mice (**C**). $^{**}P < 0.01$. $n = 3$. Scale bar, 10 µm. (**D–F**) Retinas were collected from control and diabetic mice after 6 months of DB, and retinal trypsin digestion was performed. Representative examples of periodic acid-Schiff– and hematoxylin–stained retinal trypsin digests are shown. The *red arrows* indicate pericytes, identified by morphologic criteria (shape and relative position in the capillary), and the *yellow arrows* indicate acellular capillaries. Graphs represent the number of pericytes and acellular capillaries relative to the control. $^{****}P < 0.0001$. $n = 5$.

Investigative Ophthalmology & Visual Science

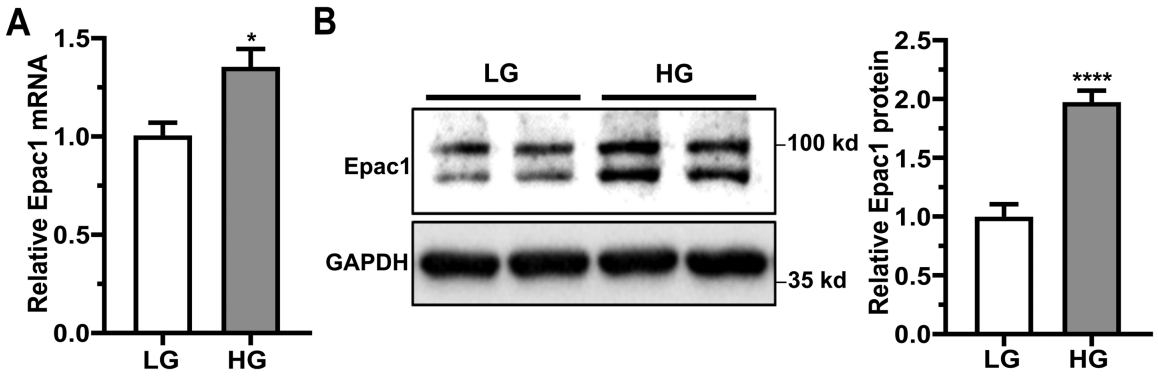

Figure 4. HG increases Epac1 expression in HRPCs. (**A**) Expression of Epac1 mRNA in HRPCs after incubation in LG or HG for 16 hours ($n = 4$). (**B**) Western blot images and quantification of Epac1 expression after LG and HG treatment for 24 hours ($n = 6$). *$P < 0.05$; ****$P < 0.0001$.

(Figs. 3A, B). Retinal vasculature mainly includes pericytes and ECs, which can be distinguished by nuclear morphology and location. The nuclei of ECs are oval or elongated and lie within the vessel wall while the nuclei of pericytes are relatively round and reside on the outer layer of the vessel wall.[48,49] After close examination, we found that Epac1 was upregulated in both ECs and pericytes of the diabetic retina (Figs. 3A–C). Six months after DB induction, DB mice exhibited a significant decrease in pericytes and an increase in acellular capillary formation (Figs. 3D–F). These results from the IR and DR models suggest a potential role of Epac1 in retinal pathogenesis, particularly pericyte loss, during ischemic retinopathy.

Epac1 Is Upregulated in HRPCs in Response to HG

To investigate potential mechanisms underlying Epac1-mediated pericyte loss, we treated primary HRPCs with HG to mimic one of the stress conditions associated with ischemic retinopathy. We cultured primary HRPCs in 5 mM glucose (LG) and then challenged them with 25 mM glucose (HG). As shown in Figure 4, the expression levels of both Epac1 mRNA and protein were upregulated significantly in HG. Two Epac1 protein bands, corresponding with the Epac1A (923 AAs) and Epac1B (881 AAs) splice variants, could be detected in HRPCs, which were further validated by full-length RT-PCR products using a cDNA library generated from HRPCs (Supplementary Fig. S3A). In contrast, the levels of Epac1 were unaltered under an osmotic control condition of 25 mM L-glucose (Supplementary Fig. S3B). These results are consistent with previous findings that hyperglycemia stimulates the transcription and translation of Epac1 in renal tubules.[43] In contrast with increased Epac1 expression, the levels of intracellular cAMP concentration remained unchanged in response to HG treatment (Supplementary Fig. S4).

Epac1 Promotes Mitochondrial Fission and ROS Production in HRPCs in Response to HG Stimulation

Our recent study shows that Epac1 promotes vascular smooth muscle cell phenotypic switching via enhancing mitochondrial fission and ROS production in response to vascular injury.[19] To investigate if Epac1 may play a similar role in pericyte injury during DR development, we monitored changes in mitochondrial morphology and ROS production in HRPCs in response to HG using Mito-Tracker and dihydroethidium. As shown in Figure 5, HG treatment induced significant mitochondrial fission in HRPCs, and pharmacological inhibition of Epac using an Epac-specific inhibitor ESI-09 (5 μM) blocked HG-induced mitochondrial fragmentation. Mitochondrial fission has been shown to contribute to hyperglycemia-induced ROS production.[50–52] Consistent with this notion, silencing Epac1 via siRNA blocked the HG-induced increase in ROS production (Fig. 6, Supplementary Fig. S5). These results suggest that HG-induced Epac1 upregulation is functionally important for HG-mediated mitochondrial fission, and that Epac1 signaling mediates HG-induced ROS production in HRPCs.

Epac1 Inhibition Suppresses HG-induced Drp1 Phosphorylation and Caspase 3 Activation in HRPCs

Members of the dynamin family of GTPases mediate mitochondrial fission and fusion, and dynamin-related protein 1 (Drp1) is the master regulator of mitochondrial division in eukaryotic organisms. Drp1 phosphorylation at serine 616 increases mitochondrial fission, whereas phosphorylation at serine 637 inhibits fission.[53] Our previous study showed that Epac1 promotes mitochondrial fission by activating Drp1 S616 phosphorylation in vascular smooth muscle cells.[19] Consistent with mitochondrial morphology analyses, we found that Drp1 phosphorylation at S616 increased significantly in HG-stimulated HRPCs, while the total Drp1 levels were unaffected (Fig. 7). In contrast, 25 mM L-glucose treatment did not affect Drp1 S616 phosphorylation (Supplementary Fig. S6). Moreover, pretreating HRPCs with ESI-09 completely blocked HG-induced Drp1 S616 phosphorylation (Figs. 7A, C). Gene silencing using siRNA specific for Epac1 also obliterated HG-induced Drp1 S616 phosphorylation (Figs. 7B, D). These results suggest that HG induces pericyte mitochondrial fission and promotes Drp1 phosphorylation at serine 616 and that inhibition of Epac1 suppresses HG-mediated mitochondrial fission and reduces

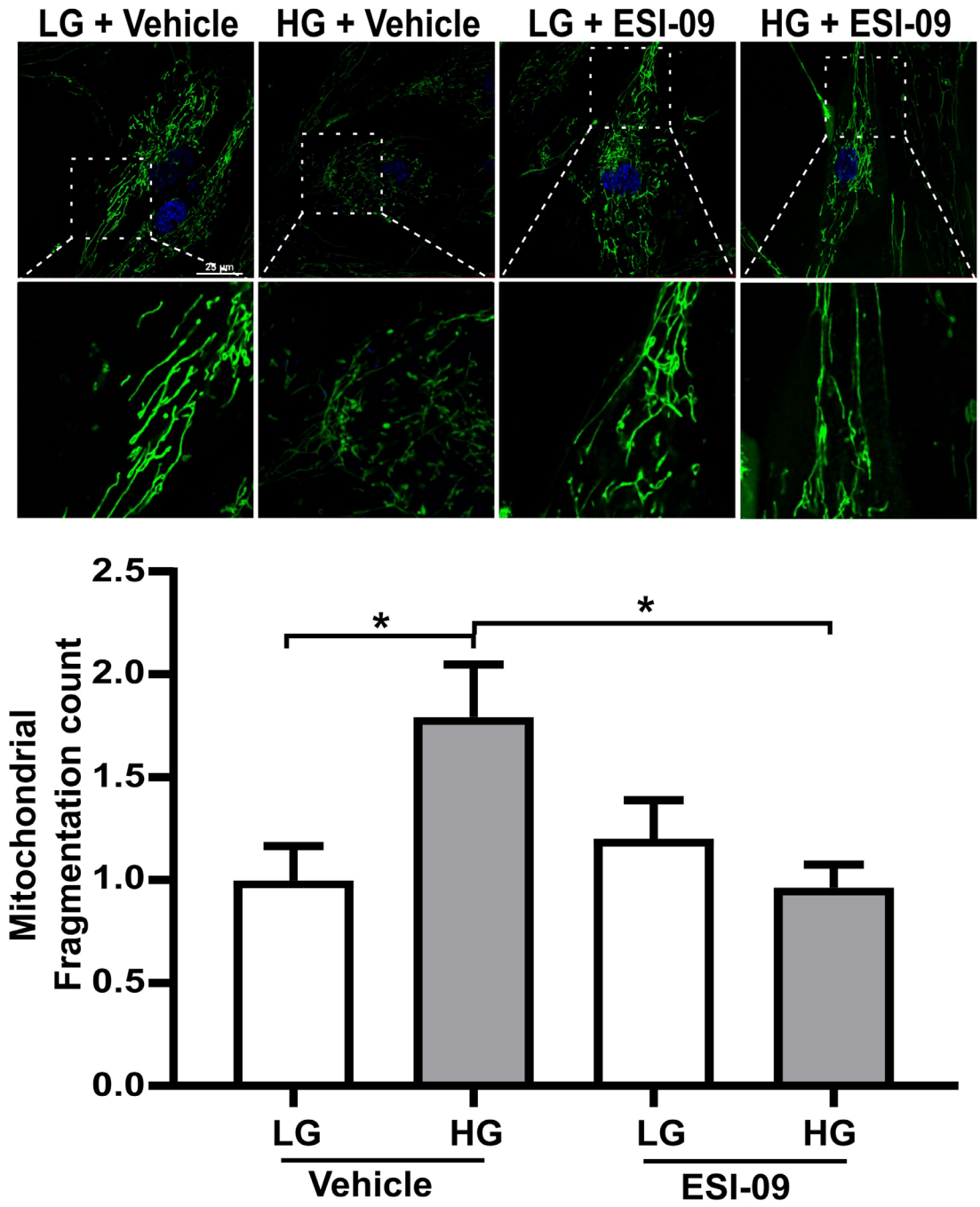

Figure 5. Epac1 inhibition suppresses HG-induced mitochondrial fission. Confocal images of mitochondrial morphology (*green*) in HRPCs treated with vehicle or ESI-09 in the presence of LG or HG for 1.5 hours. Quantification of mitochondrial fission is shown as mitochondrial fragmentation count. *$P < 0.05$. $n = 5$–6. Scale bar, 25 μm.

Drp1 S616 phosphorylation. Mitochondrial fission plays a critical role in programmed cell death.[54,55] To determine if Epac1 is involved in HG-induced HRPC apoptosis, we incubated HRPCs in HG and monitored caspase 3 activation by assessing the level of cleaved caspase 3. As shown in Figure 8, HG treatment induced caspase 3 activation in HRPCs, which was blocked by pharmacological inhibition or gene silencing of Epac1. Taken together, our data support the notion that Epac1 is an important stress response signal that regulates mitochondrial dynamics, ROS production, and apoptosis in HRPCs under stress conditions.

Discussion

Pericytes are important in maintaining retinal blood vessels' structural and functional integrity. In this study, we focused on probing the role of Epac1 signaling in pericyte degeneration during retinal vascular injury. Our current study reveals that IR-induced retinal capillary degeneration is associated with an increased expression of Epac1 in the mouse retinal vasculature, including both ECs and pericytes. Similarly, we find that the levels of Epac1 expression, pericyte loss, and acellular capillary formation are also increased in the retinal

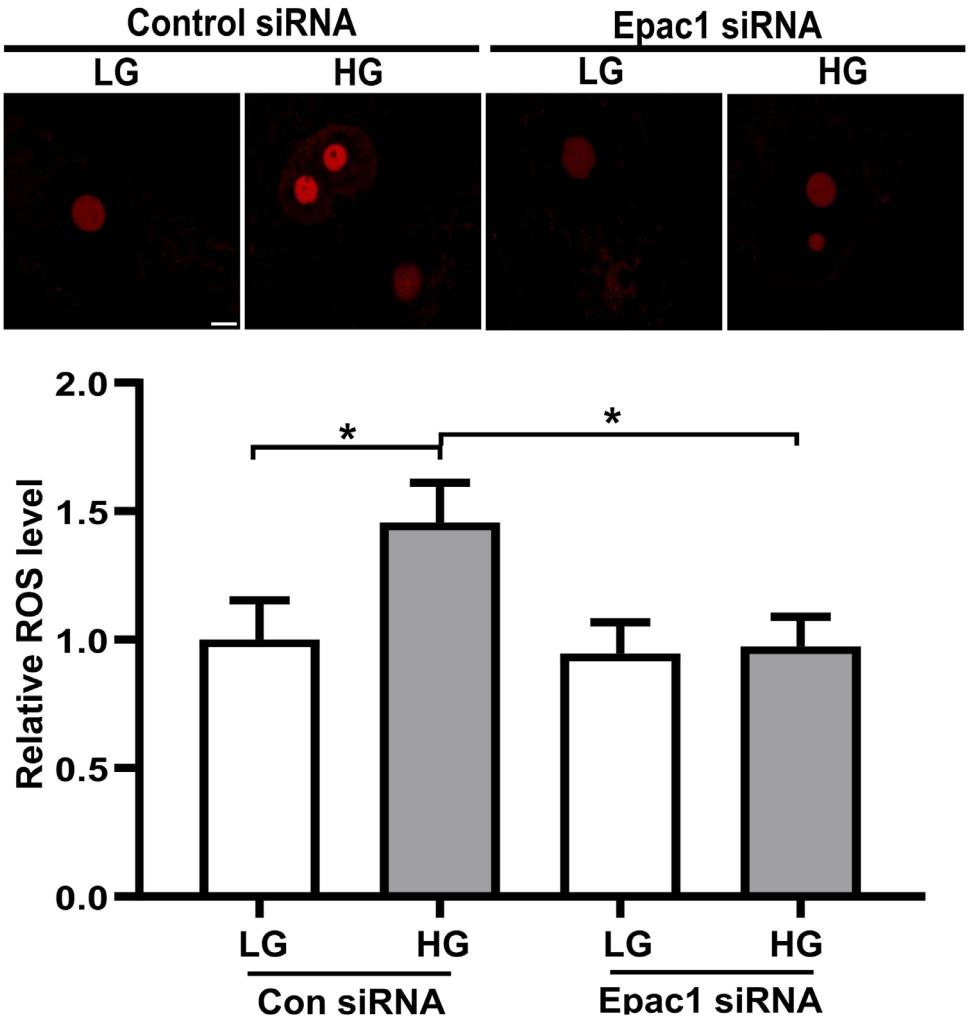

Figure 6. Silencing of Epac1 suppresses HG-induced mitochondrial ROS production. Confocal images of ROS levels detected with DHE staining (*red*) in HRPCs transfected with control or Epac1-specific siRNA and cultured in LG or HG for 1 hour. The graph indicates the quantification of the relative ROS levels. *$P < 0.05$. $n \geq 14$. Scale bar, 5 µm.

vasculature of diabetic mice. Deletion of Epac1 significantly decreased IR-induced formation of acellular capillaries and pericyte loss. These data suggest that Epac1 contributes to vascular degeneration and pericyte injury during ischemic retinopathy. Work is currently ongoing to determine the effects of Epac1 deletion on pericyte injury and capillary degeneration in STZ-induced DB.

Consistent with in vivo expression status, Epac1 levels in HRPCs are also upregulated in response to HG stimulation. These results likely reflect the fact that the Epac1 promoter contains two glucose-responsive element sites and two E-box motifs known to be important for glucose responsiveness.[43] HG-induced Epac1 expression in pericytes is accompanied by increased Drp1 phosphorylation, mitochondrial fission, ROS production, and caspase 3 activation. Conversely, inhibition of Epac1 expression via RNA interference or activity via a pharmacological approach effectively blocks HG-mediated mitochondrial dysfunction and caspase 3 activation. These results support the notion that Epac1 contributes to the development of ischemic retinopathy by inducing pericyte loss via modulating mitochondrial fission/ROS production under HG conditions. Besides energy production, the mitochondria play crucial roles in other important cellular processes, such as Ca^{2+} buffering, ROS production, and apoptosis. Extensive studies have demonstrated that mitochondrial dynamics, particularly fission, actively participate in apoptosis induction.[54,56,57] Multiple reports, including those from our laboratory, have shown that deletion of Epac1 in mice protects against stress-induced mitochondrial dysfunction and cell death in various tissues, including cardiomyocytes,[40,58] vascular smooth muscle cells,[19] and neurons.[59,60] Results from this study suggest that genetic deletion of Epac1 protects from pericyte loss and formation of acellular capillaries in ischemic retinopathy, thus further expanding this list to include the retina.

Our current studies demonstrate that Epac1 plays a pathological role in pericyte dysfunction and vascular degeneration during ischemic retinopathy. A previous study showed that tissue-specific deletion of Epac1 in ECs accelerated IR-induced neuronal and vascular damage.[61] Although the exact reasons for this apparent discrepancy are unclear, as noted in our previous study in which Epac1 deletion preserved retinal neuronal function,[33] we used mice with a pure C57BL/6 background in this study. In contrast, the abovementioned study used mice on mixed backgrounds

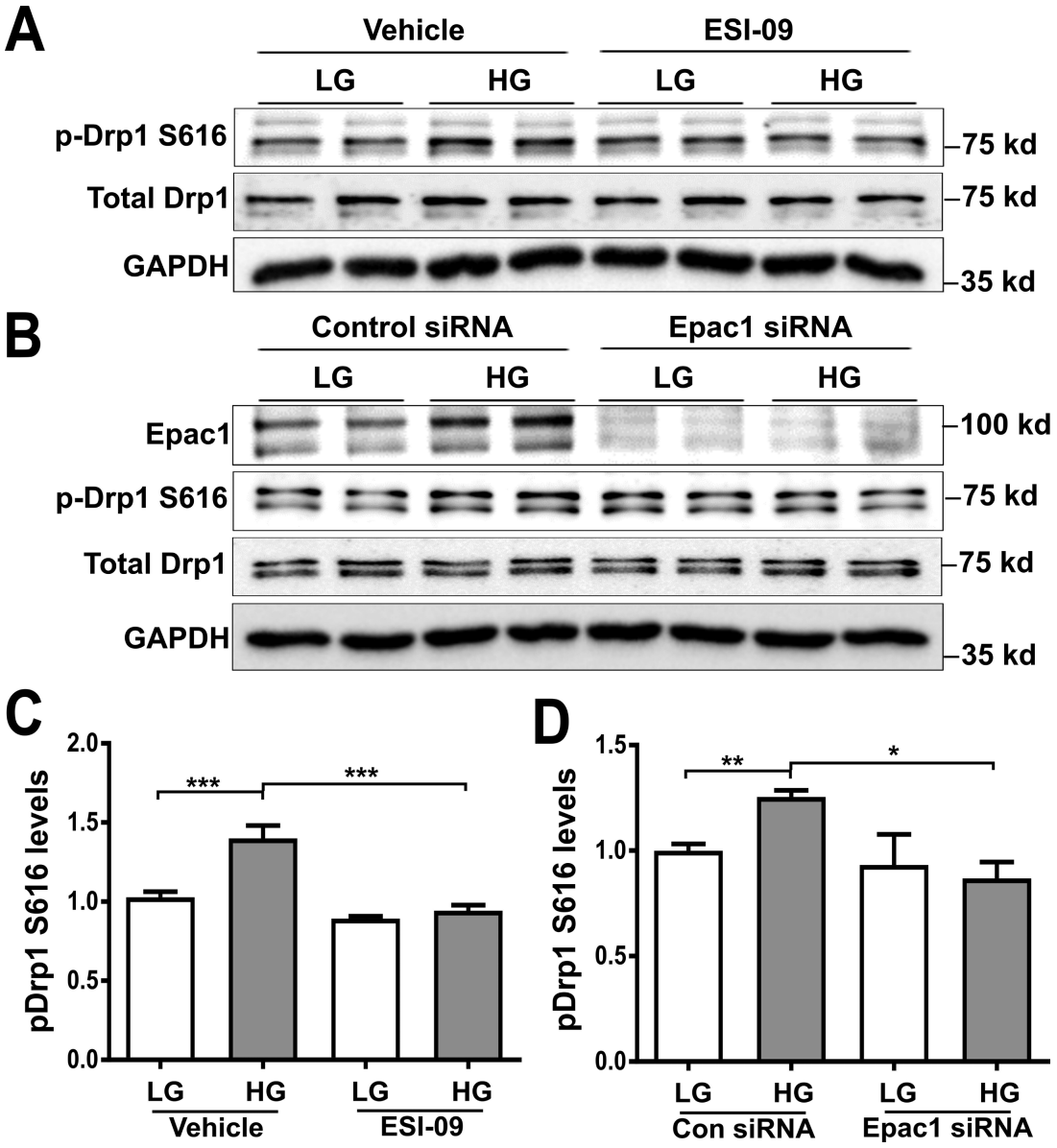

Figure 7. Epac1 inhibition suppresses HG-induced Drp1 phosphorylation. (**A**, **C**) Western blot images and quantification of p-DRP1 S616 and total Drp1 in HRPCs cultured in LG or HG for 16 hours and pretreated with vehicle or ESI-09. (**B**, **D**) Western blot images and quantification of p-DRP1 S616 and total Drp1 in HRPCs transfected with control or Epac1-specific siRNA and cultured in LG or HG for 16 hours. $^{*}P < 0.05$; $^{**}P < 0.01$; $^{***}P < 0.0005$. $n \geq 4$.

of B6/129S, which are more prone to variability. Therefore, the discrepancy could be due to the different genetic backgrounds of the used mouse strains. Another difference in experimental design between the studies was in the types of mouse models used, namely, a whole body Epac1 KO model versus an endothelial tissue-specific Epac1 KO model. Epac1 may exert different functions in different tissue/cell types, contributing to the apparent discrepancy.

Although the Epac1 global KO mouse model is essential for characterizing the general phenotype of Epac1 deletion and investigating its effects in systemic diseases, it has several potential limitations, including complications owing to possible perturbation of embryonic development and lack of tissue-specific insights. Our previous studies have demonstrated that Epac1 is not essential for mouse development in general[32] and for the formation of retinal vasculature,[21] eliminating the developmental issue. However, a potential limitation of our current study is that, in addition to pericytes, Epac1 is expressed in other cell types, such as macrophages within the retinal vasculature. This factor could also contribute to pericyte dysfunction. Additional studies using tissue-specific Epac1 KO mouse models are necessary to sort this out. Indeed, our previous study using a myeloid-specific Epac1 deletion model showed that Epac1 in macrophages is dispensable for IR-induced retinal neurodegeneration.[33] We have also generated endothelial- and pericyte-specific Epac1 KO models. These tissue-specific Epac1 KO models will allow us to determine the contributions of Epac1 in specific populations of resident retinal cells to vascular degeneration and pericyte injury in ischemic retinopathy.

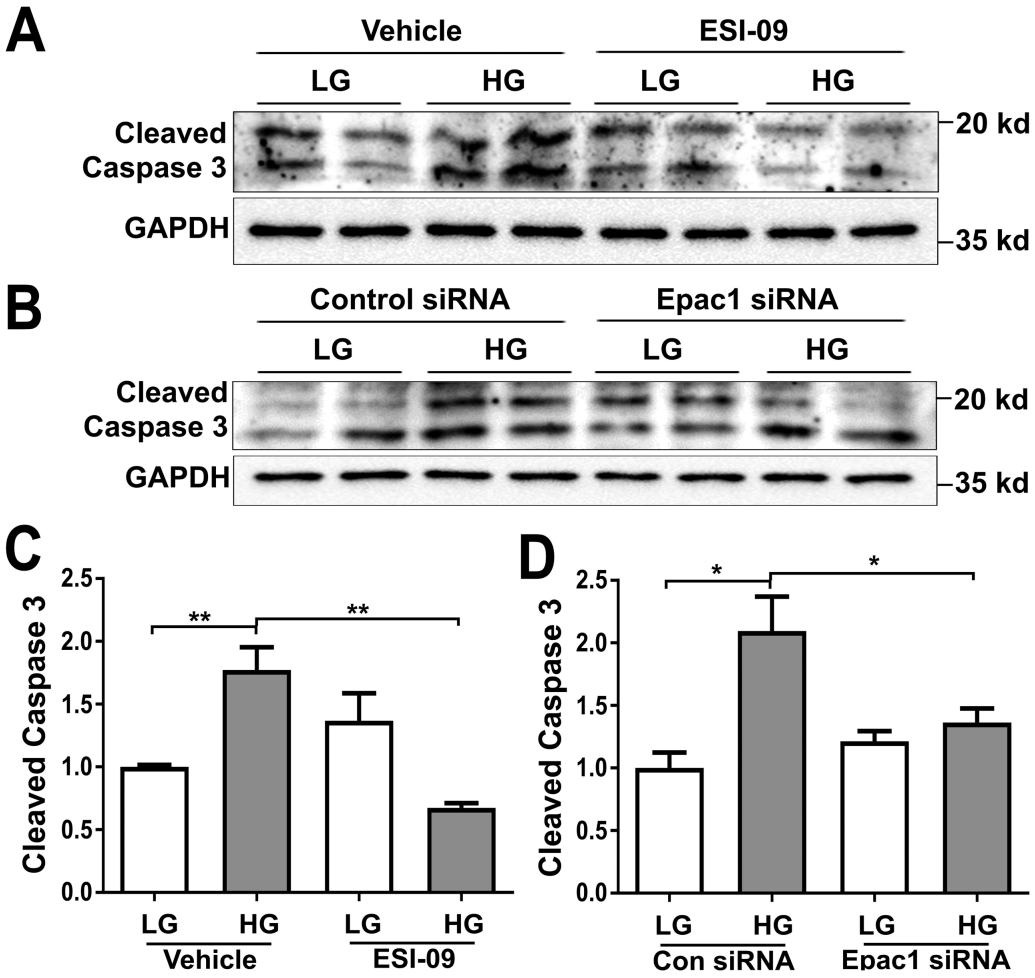

Figure 8. Epac1 inhibition suppresses HG-induced caspase 3 activation. (**A**, **C**) Western blot images and quantification of cleaved caspase 3 in HRPCs cultured in LG or HG for 16 hours and pretreated with vehicle or ESI-09. (**B**, **D**) Western blot images and quantification of cleaved caspase 3 in HRPCs transfected with control or Epac1-specific siRNAs and cultured in LG or HG for 24 hours. $^{*}P < 0.05$; $^{**}P < 0.01$. $n = 4$.

Acknowledgments

The authors thank Olga Chumakova at the Center for Advanced Microscopy for assistance in microscopic imaging and Jeffery Frost for the critical review of the manuscript.

Supported by grants from the National Institutes of Health R01EY033319 (X.C. and H.L.) and R01EY022694 (W.Z.).

Disclosure: **W. Yang**, None, **F. Xia**, None; **F. Mei**, None; **S. Shi**, None; **W.G. Robichaux III**, None; **W. Lin**, None; **W. Zhang**, None; **H. Liu**, None; **X. Cheng**, None

References

1. Cheung N, Mitchell P, Wong TY. Diabetic retinopathy. *Lancet*. 2010;376(9735):124–136.
2. Gutsaeva DR, Shalaby L, Powell FL, et al. Inactivation of endothelial ADAM17 reduces retinal ischemia-reperfusion induced neuronal and vascular damage. *Int J Mol Sci*. 2020;21(15):5379.
3. Klotzsche-von Ameln A, Sprott D. Harnessing retinal phagocytes to combat pathological neovascularization in ischemic retinopathies? *Pflugers Arch*. 2022;474(6):575–590.
4. Shosha E, Xu Z, Yokota H, et al. Arginase 2 promotes neurovascular degeneration during ischemia/reperfusion injury. *Cell Death Dis*. 2016;7(11):e2483.
5. Wei Y, Gong J, Yoshida T, et al. Nrf2 has a protective role against neuronal and capillary degeneration in retinal ischemia-reperfusion injury. *Free Radic Biol Med*. 2011;51(1):216–224.
6. Narayanan SP, Rojas M, Suwanpradid J, Toque HA, Caldwell RW, Caldwell RB. Arginase in retinopathy. *Prog Retin Eye Res*. 2013;36:260–280.
7. ValdezGuerrero AS, Quintana-Perez JC, Arellano-Mendoza MG, Castaneda-Ibarra FJ, Tamay-Cach F, Aleman-Gonzalez-Duhart D. Diabetic retinopathy: important biochemical alterations and the main treatment strategies. *Can J Diabetes*. 2020;45(6):604–511.
8. Duh EJ, Sun JK, Stitt AW. Diabetic retinopathy: current understanding, mechanisms, and treatment strategies. *JCI Insight*. 2017;2(14):e93751.
9. Cheng X, Ji Z, Tsalkova T, Mei F. Epac and PKA: a tale of two intracellular cAMP receptors. *Acta Biochim Biophys Sin (Shanghai)*. 2008;40(7):651–662.
10. de Rooij J, Zwartkruis FJ, Verheijen MH, et al. Epac is a Rap1 guanine-nucleotide-exchange factor directly activated by cyclic AMP. *Nature*. 1998;396(6710):474–477.

Investigative Ophthalmology & Visual Science

11. Kawasaki H, Springett GM, Mochizuki N, et al. A family of cAMP-binding proteins that directly activate Rap1. *Science*. 1998;282(5397):2275–2279.
12. Schmidt M, Dekker FJ, Maarsingh H. Exchange protein directly activated by cAMP (epac): a multidomain cAMP mediator in the regulation of diverse biological functions. *Pharmacol Rev*. 2013;65(2):670–709.
13. Banerjee U, Cheng X. Exchange protein directly activated by cAMP encoded by the mammalian rapgef3 gene: structure, function and therapeutics. *Gene*. 2015;570(2):157–167.
14. Sugawara K, Shibasaki T, Takahashi H, Seino S. Structure and functional roles of Epac2 (Rapgef4). *Gene*. 2016;575(2 Pt 3):577–583.
15. Robichaux WG, 3rd, Cheng X. Intracellular cAMP sensor EPAC: physiology, pathophysiology, and therapeutics development. *Physiol Rev*. 2018;98(2):919–1053.
16. Roberts OL, Dart C. cAMP signalling in the vasculature: the role of Epac (exchange protein directly activated by cAMP). *Biochem Soc Trans*. 2014;42(1):89–97.
17. Yokoyama U, Minamisawa S, Quan H, et al. Epac1 is upregulated during neointima formation and promotes vascular smooth muscle cell migration. *Am J Physiol Heart Circ Physiol*. 2008;295(4):H1547–1555.
18. Kato Y, Yokoyama U, Yanai C, et al. Epac1 deficiency attenuated vascular smooth muscle cell migration and neointimal formation. *Arterioscler Thromb Vasc Biol*. 2015;35(12):2617–2625.
19. Wang H, Robichaux WG, Wang Z, et al. Inhibition of Epac1 suppresses mitochondrial fission and reduces neointima formation induced by vascular injury. *Sci Rep*. 2016;6:36552.
20. Robichaux WG, 3rd, Mei FC, Yang W, et al. Epac1 (exchange protein directly activated by cAMP 1) upregulates LOX-1 (oxidized low-density lipoprotein receptor 1) to promote foam cell formation and atherosclerosis development. *Arterioscler Thromb Vasc Biol*. 2020;40(12):e322–e335.
21. Liu H, Mei FC, Yang W, et al. Epac1 inhibition ameliorates pathological angiogenesis through coordinated activation of Notch and suppression of VEGF signaling. *Sci Adv*. 2020;6(1):eaay3566.
22. Orlidge A, D'Amore PA. Inhibition of capillary endothelial cell growth by pericytes and smooth muscle cells. *J Cell Biol*. 1987;105(3):1455–1462.
23. von Tell D, Armulik A, Betsholtz C. Pericytes and vascular stability. *Exp Cell Res*. 2006;312(5):623–629.
24. Hammes HP, Lin J, Renner O, et al. Pericytes and the pathogenesis of diabetic retinopathy. *Diabetes*. 2002;51(10):3107–3112.
25. Hammes HP, Lin J, Wagner P, et al. Angiopoietin-2 causes pericyte dropout in the normal retina: evidence for involvement in diabetic retinopathy. *Diabetes*. 2004;53(4):1104–1110.
26. Hammes HP. Pericytes and the pathogenesis of diabetic retinopathy. *Horm Metab Res*. 2005;37(Suppl 1):39–43.
27. Beltramo E, Porta M. Pericyte loss in diabetic retinopathy: mechanisms and consequences. *Curr Med Chem*. 2013;20(26):3218–3225.
28. Pfister F, Przybyt E, Harmsen MC, Hammes HP. Pericytes in the eye. *Pflugers Arch*. 2013;465(6):789–796.
29. Trudeau K, Molina AJ, Guo W, Roy S. High glucose disrupts mitochondrial morphology in retinal endothelial cells: implications for diabetic retinopathy. *Am J Pathol*. 2010;177(1):447–455.
30. Trudeau K, Molina AJ, Roy S. High glucose induces mitochondrial morphology and metabolic changes in retinal pericytes. *Invest Ophthalmol Vis Sci*. 2011;52(12):8657–8664.
31. Tien T, Zhang J, Muto T, Kim D, Sarthy VP, Roy S. High glucose induces mitochondrial dysfunction in retinal Muller cells: implications for diabetic retinopathy. *Invest Ophthalmol Vis Sci*. 2017;58(7):2915–2921.
32. Yan J, Mei FC, Cheng H, et al. Enhanced leptin sensitivity, reduced adiposity, and improved glucose homeostasis in mice lacking exchange protein directly activated by cyclic AMP isoform 1. *Mol Cell Biol*. 2013;33(5):918–926.
33. Liu W, Ha Y, Xia F, et al. Neuronal Epac1 mediates retinal neurodegeneration in mouse models of ocular hypertension. *J Exp Med*. 2020;217(4):e20190930.
34. Rojas M, Zhang W, Xu Z, et al. Requirement of NOX2 expression in both retina and bone marrow for diabetes-induced retinal vascular injury. *PLoS One*. 2013;8(12):e84357.
35. Saadane A, Lessieur EM, Du Y, Liu H, Kern TS. Successful induction of diabetes in mice demonstrates no gender difference in development of early diabetic retinopathy. *PLoS One*. 2020;15(9):e0238727.
36. Rehman J, Zhang HJ, Toth PT, et al. Inhibition of mitochondrial fission prevents cell cycle progression in lung cancer. *Faseb J*. 2012;26(5):2175–2186.
37. Almahariq M, Mei FC, Cheng X. The pleiotropic role of exchange protein directly activated by cAMP 1 (EPAC1) in cancer: implications for therapeutic intervention. *Acta Biochim Biophys Sin (Shanghai)*. 2016;48(1):75–81.
38. Okumura S, Fujita T, Cai W, et al. Epac1-dependent phospholamban phosphorylation mediates the cardiac response to stresses. *J Clin Invest*. 2014;124(6):2785–2801.
39. Métrich M, Lucas A, Gastineau M, et al. Epac mediates beta-adrenergic receptor-induced cardiomyocyte hypertrophy. *Circ Res*. 2008;102(8):959–965.
40. Fazal L, Laudette M, Paula-Gomes S, et al. Multifunctional mitochondrial Epac1 controls myocardial cell death. *Circ Res*. 2017;120(4):645–657.
41. Wang H, Heijnen CJ, van Velthoven CT, et al. Balancing GRK2 and EPAC1 levels prevents and relieves chronic pain. *J Clin Invest*. 2013;123(12):5023–5034.
42. Eijkelkamp N, Linley JE, Torres JM, et al. A role for Piezo2 in EPAC1-dependent mechanical allodynia. *Nat Commun*. 2013;4:1682.
43. Sun L, Kondeti VK, Xie P, Raparia K, Kanwar YS. Epac1-mediated, high glucose-induced renal proximal tubular cells hypertrophy via the Akt/p21 pathway. *Am J Pathol*. 2011;179(4):1706–1718.
44. Zheng L, Gong B, Hatala DA, Kern TS. Retinal ischemia and reperfusion causes capillary degeneration: similarities to diabetes. *Invest Ophthalmol Vis Sci*. 2007;48(1):361–367.
45. Hartsock MJ, Cho H, Wu L, Chen WJ, Gong J, Duh EJ. A mouse model of retinal ischemia-reperfusion injury through elevation of intraocular pressure. *J Vis Exp*. 2016;14(113):54065.
46. Lai TW, Lin SZ, Lee HT, et al. HIF-1α binding to the Epac1 promoter recruits hematopoietic stem cells to the ischemic brain following stroke. *J Mol Cell Biol*. 2012;4(3):184–187.
47. Lin CH, Lee HT, Lee SD, et al. Role of HIF-1α-activated Epac1 on HSC-mediated neuroplasticity in stroke model. *Neurobiol Dis*. 2013;58:76–91.
48. Dietrich N, Hammes HP. Retinal digest preparation: a method to study diabetic retinopathy. *Methods Mol Biol*. 2012;933:291–302.
49. Han WH, Gotzmann J, Kuny S, et al. Modifications in retinal mitochondrial respiration precede type 2 diabetes and protracted microvascular retinopathy. *Invest Ophthalmol Vis Sci*. 2017;58(10):3826–3839.
50. Yu T, Robotham JL, Yoon Y. Increased production of reactive oxygen species in hyperglycemic conditions requires dynamic change of mitochondrial morphology. *Proc Natl Acad Sci USA*. 2006;103(8):2653–2658.

Investigative Ophthalmology & Visual Science

51. Yu T, Sheu SS, Robotham JL, Yoon Y. Mitochondrial fission mediates high glucose-induced cell death through elevated production of reactive oxygen species. *Cardiovasc Res*. 2008;79(2):341–351.
52. Yu T, Jhun BS, Yoon Y. High-glucose stimulation increases reactive oxygen species production through the calcium and mitogen-activated protein kinase-mediated activation of mitochondrial fission. *Antioxid Redox Signal*. 2011;14(3):425–437.
53. van der Bliek AM, Shen Q, Kawajiri S. Mechanisms of mitochondrial fission and fusion. *Cold Spring Harb Perspect Biol*. 2013;5(6):a011072.
54. Suen DF, Norris KL, Youle RJ. Mitochondrial dynamics and apoptosis. *Genes Dev*. 2008;22(12):1577–1590.
55. Youle RJ, Karbowski M. Mitochondrial fission in apoptosis. *Nat Rev Mol Cell Biol*. 2005;6(8):657–663.
56. Martinou JC, Youle RJ. Mitochondria in apoptosis: Bcl-2 family members and mitochondrial dynamics. *Dev Cell*. 2011;21(1):92–101.
57. Ugarte-Uribe B, García-Sáez AJ. Membranes in motion: mitochondrial dynamics and their role in apoptosis. *Biol Chem*. 2014;395(3):297–311.
58. Lezoualc'h F, Fazal L, Laudette M, Conte C. Cyclic AMP sensor EPAC proteins and their role in cardiovascular function and disease. *Circ Res*. 2016;118(5):881–897.
59. Singhmar P, Huo X, Li Y, et al. Orally active Epac inhibitor reverses mechanical allodynia and loss of intraepidermal nerve fibers in a mouse model of chemotherapy-induced peripheral neuropathy. *Pain*. 2018;159(5):884–893.
60. Jakobsen E, Lange SC, Bak LK. Soluble adenylyl cyclase-mediated cAMP signaling and the putative role of PKA and EPAC in cerebral mitochondrial function. *J Neurosci Res*. 2019;97(8):1018–1038.
61. Liu L, Jiang Y, Steinle JJ. Epac1 protects the retina against ischemia/reperfusion-induced neuronal and vascular damage. *PLoS One*. 2018;13(9):e0204346.

Investigative Ophthalmology & Visual Science